A New Concept for Primary Reconstruction of Skull Defects with 3D-Molded PEEK Patch Assisted by Navigation Based on Animal Study

Jin GONG[*1], YangJie XIE[*2], HaiYong HE[1], ManTing LI[1], Lun LUO[1], BaoYu ZHANG[1], TengChao HUANG[1], RongQian YANG[2], Ying GUO[1]

[1]Sun Yat-Sen University, The Third Affiliated Hospital of Sun Yat-Sen University, Department of Neurosurgery, Guangzhou, Guangdong Province, P.R. China
[2]South China University of Technology, Department of Biomedical Engineering, Guangzhou, Guangdong Province, P.R. China

*Authors contributed equally to this work.

Corresponding author: Ying GUO ✉ guoy@mail.sysu.edu.cn

ABSTRACT

AIM: To perform an accurate primary repair of temporal bone defects.

MATERIAL and METHODS: The temporal bone defect models were performed in beagles. Extended estimated patches of the defects were predesigned by 3D reconstruction software and molded from polyether ether ketone (PEEK) using a lathe. The precise trimming of the extended PEEK patches was established via coordinate transformation of the patches between the navigation system and the reconstruction software, and in real-time tracing via intraoperative navigation. Trimmed PEEK patches were embedded onto the defects. Blood tests and image examinations were conducted postoperatively.

RESULTS: The extended PEEK patches were prepared precisely according to the predesign. Real-time tracing of the actual skull defect profile was performed quickly and accurately. Trimmed skull patches perfectly matched the shape of the defects. No signs of infection, absorption, or translocation of the patches occurred postoperatively, and little epidural effusion was found.

CONCLUSION: With the assistance of navigation and 3D reconstruction technology, customized molded PEEK patches can be used for accurate primary repair of temporal bone defects.

KEYWORDS: Temporal bone defect, Skull reconstruction, Polyether ether ketone patch, Navigation, Molding

INTRODUCTION

Temporal bone tumors, such as benign osteoma and malignant squamous cell carcinoma, require primary repair after lesion resection. Although cranioplasty techniques are well established, reconstruction of the temporal bone defect adjacent to the skull base remains a challenge for neurosurgeons. Matching problems involving the repair material and the skull defect after repair, particularly in the lower part of temporal bone, may result in overlying scalp atrophy (10), implant exposure, (20) and sunk tempora, which is unacceptable to many young people. Although 3D molding technology has made it possible to duplicate the perfect exact shape of the defect with titanium (Ti) mesh or polyether ether ketone (PEEK), it is difficult to obtain satisfactory results during primary osseous reconstruction, particularly in temporal bone tumor resection. The biggest problem is the inability to accurately predict the intraoperative craniectomy range before surgery. Ti mesh and polymethyl methacrylate (PMMA) are widely used to repair defects in the skull base, but

Jin GONG (iD): 0000-0002-0059-8087
YangJie XIE (iD): 0000-0002-8343-3949
HaiYong HE (iD): 0000-0002-5180-926X
ManTing LI (iD): 0000-0002-0230-5540
Lun LUO (iD): 0000-0002-6765-336X
BaoYu ZHANG (iD): 0000-0001-9450-4258
TengChao HUANG (iD): 0000-0001-7030-5852
RongQian YANG (iD): 0000-0001-7864-2677
Ying GUO (iD): 0000-0001-7105-002X

unsatisfactory effects often occur due to hard cutting, metal artifacts, heat production, self-absorption, infection, etc. The development of 3D molding technologies has made it possible to use personalized skull patches made of polymer materials in clinical applications (11,21). However, the intraoperative mismatch between the patch and the defect and difficulties with immobilization significantly hamper its use in clinical settings. Due to its superior physicochemical properties and lack of image artifacts, PEEK is often used in cranioplasty (14,17). With the aid of novel lathe technology, PEEK can be used to form complex 3D skull base structures. Based on this, we present a novel method to manufacture adaptive, personalized PEEK patches that combines 3D molding, intraoperative navigation, and real-time 3D reconstruction technology. Animal experiments were performed to verify the feasibility of the clinical application of this method in accurate primary osseous reconstruction of skull base defects.

■ MATERIAL and METHODS

Animals

Six beagles of mixed gender aged 1.5–2 years and weighing 12–15 kg were approved by the Ethical Committee for Animals. All dogs were housed individually in standard cages under ambient temperatures of 20–25°C, with a relative humidity of 30–70%.

Computed Tomography (CT) Scan and Repair Patch 3D Model Reconstruction

Thin-slice images of the head (0.625 mm) with landmarks were acquired using a 120-row Siemens Dual Source Spiral CT scanner (Siemens, Munich, Germany). The Digital Imaging and Communications in Medicine (DICOM) format data were imported into the 3D Slicer software (http://www.slicer.org/), and the 3D skull model was segmented. A model of the extended repair patch with the actual outline offset inward by 1–2 cm was designed based on the estimated intraoperative defect area. Five tiny feature cylinders, 2 mm in height and 2 mm in diameter, were added onto the surface of the patch, and the center coordinates were recorded. STL (STereoLithography) and FCSV files (A CSV file reader and writer library in C/C++) containing the information for the models and coordinates were saved.

Protocol of PEEK 3D Molding

The STL file was input into the specialized processing software, and the PEEK raw material was automatically cut and polished to a specific shape by a multi-axis lathe with 3D processing ability. The theoretical machining accuracy was up to 0.005 mm.

The Process of Skull Defect Repair

Establishment of the Model of the Temporal Bone Defect

Each dog was placed in a prone position with the head fixed and was exposed to continuous endotracheal inhalation anesthesia with isoflurane after 12 hours of fasting. This was followed by navigation registration based on skin landmarks and sterilization. Then, a curved incision was made on the right temporal bone above the ear, the skin was cut and pulled outwards, and the temporal muscle was partly detached. The temporal bone was exposed, and a defect of about 2 × 3 cm was created in the skull adjoining the base using an electric drill.

Coordinate Transformation

To perform intraoperative 3D modeling for the skull base defect and patch registration, the coordinates of the dog were first mapped from the 3D slicer to the navigation. After the matrix between the 3D slicer system and the navigation system was calculated via iterative closest point (ICP) coordinate transformation, the real coordinates, including the central coordinates of the 5 tiny feature cylinders of the dog, were determined in the navigation system. The coordinates of the skull structure in the 3D slicer (PD) and the navigation system (PI), respectively, were obtained, and then the rotation and translation matrix of 2 spatial coordinates (RDI and TDI) were calculated through point set matching. Finally, the coordinates of the navigation system (PI) were obtained by the following formula: PI = RDI * PD + TDI.

Patch Registration and Implant

Patch registration

As previously noted, the profile of the skull base defect was extracted by a real-time tracking navigation probe, and an overlay was displayed on the 3D skull model. Then, the 3D-molded extended skull patch was registered by intraoperative navigation through the central coordinates of the 5 tiny feature cylinders after coordinate transformation from the 3D Slicer to the navigation system.

Patch trimming and implant

The actual profile of the defect on the extended patch was duplicated by a navigation probe according to the earlier results. Then, the patch was trimmed and implanted into the defect site. Routine nutritional support was given to the experiment animals postoperatively.

Postoperative Observation

White blood cells and C-reactive protein were examined to detect inflammation at 1, 7, and 30 days postoperation. CT and magnetic resonance imaging (MRI) scans were taken 1 month after the operation to observe the change of the patch.

The diagram of the experiment is shown in Figure 1A-H.

■ RESULTS

Through 3D reconstruction (Figure 2A-D) and lathe forming technology (Figure 3A-D), we built a personalized extended PEEK skull defect patch (Figure 4A-D). The average time for the defect estimate and the patch design from the importation of CT data to the initiation of molding was less than 30 minutes. The average molding time of the lathe process for a patch of about 2 cm × 3 cm × 0.2 cm in size was 60 minutes.

The coordinate system between the 3D Slicer and the navigation was perfectly matched after coordinate transformation (Figure 5A-F).
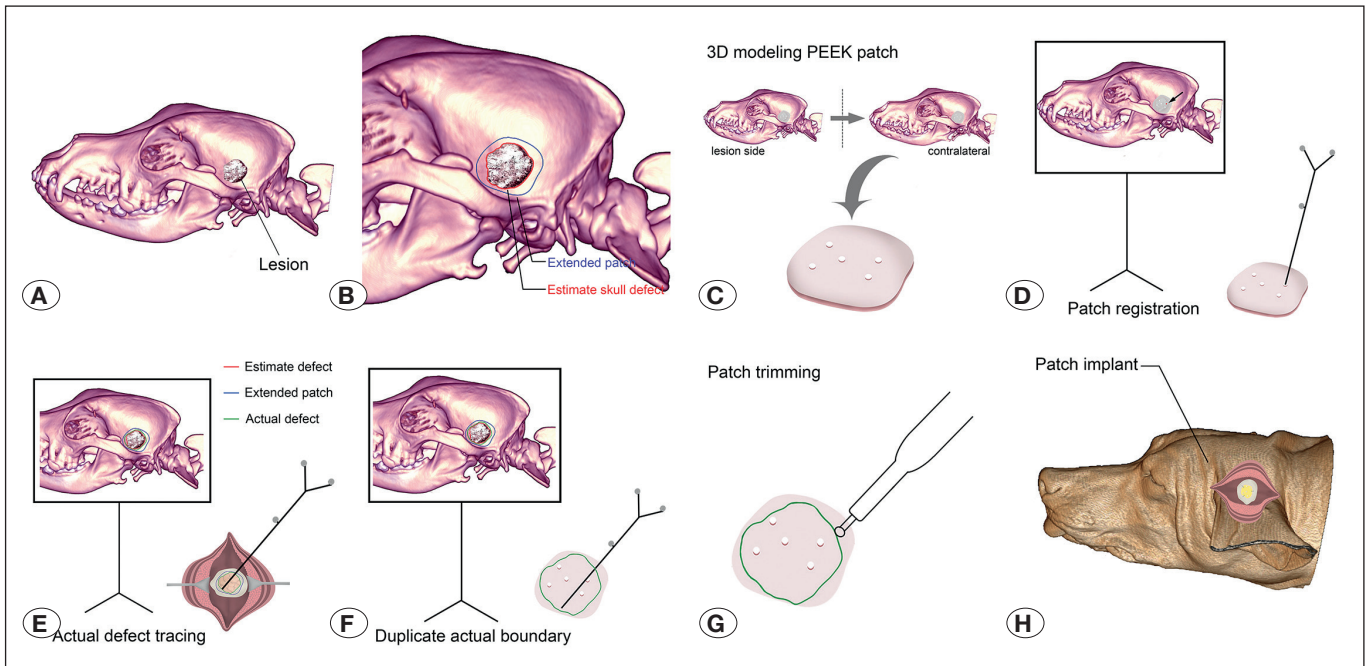
Figure 1: A novel concept of primary osseous reconstruction of the skull. **A)** Temporal bone lesion. **B)** Estimated area of the skull defects (red line) and extended area of the patch (blue line) is designed via 3D-Slicer software. **C)** A 3D extended patch model with 5 tiny feature cylinders on the surface was built according to the mirror shape of the contralateral and molded by multi-axis linkage lathe. **D)** Registration of the extended patch to the preoperative planning model through the central coordinates of the 5 tiny feature cylinders via neuronavigation. **E)** Intraoperative tracing of the actual profile of the defect (green line) by neuronavigation. **F)** Duplication of the actual profile of the defect on the extended patch (green line) by neuronavigation. **G)** Trimming the extended patch along the path by surgical drill. **H)** Implantation and fixation of the matched patch.
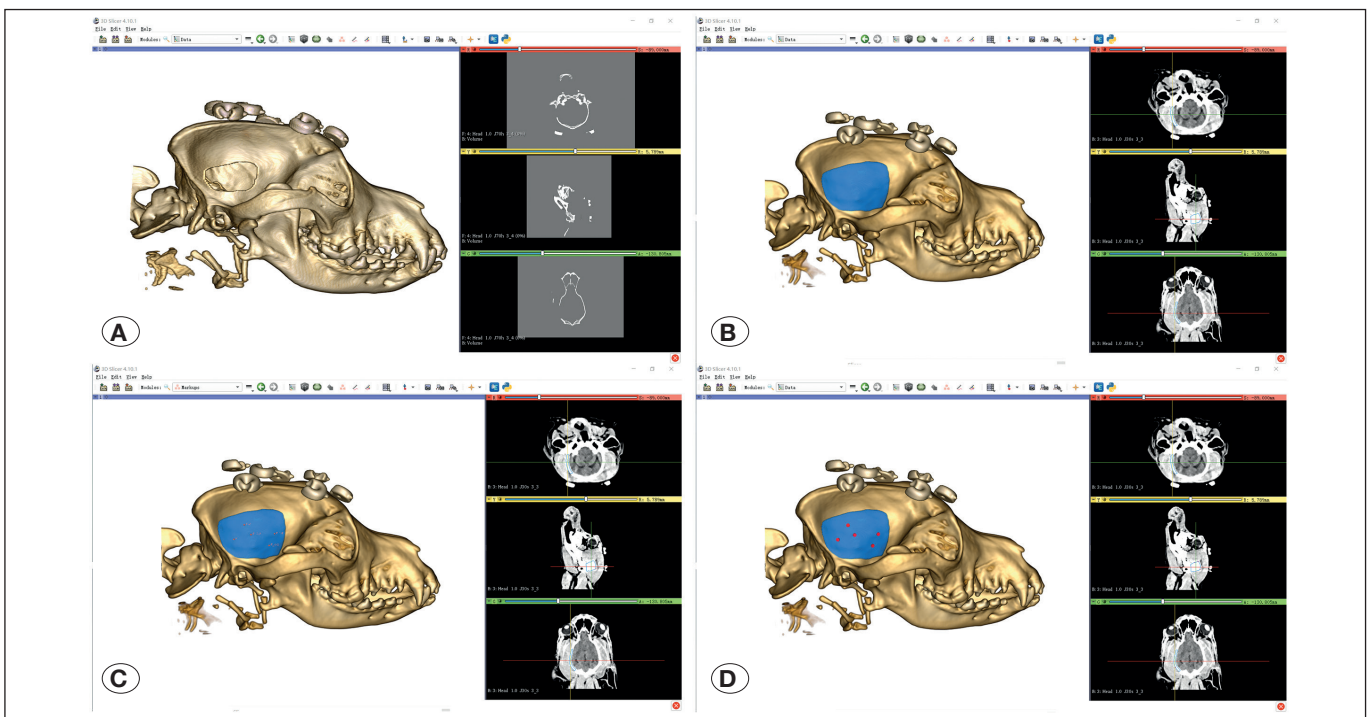

Figure 2: Preoperative simulation of the defect of the temporal bone and design of the extended patch. **A)** Estimating the defect area of the temporal bone. **B)** Design of the extended patch segment with the outline being offset outward by 1–2 cm. **C)** Set of 5 fiducial points distant on the segment. **D)** Establishment of 5 tiny feature cylinders based on previous fiducial points, 2 mm in height and 2 mm in diameter.
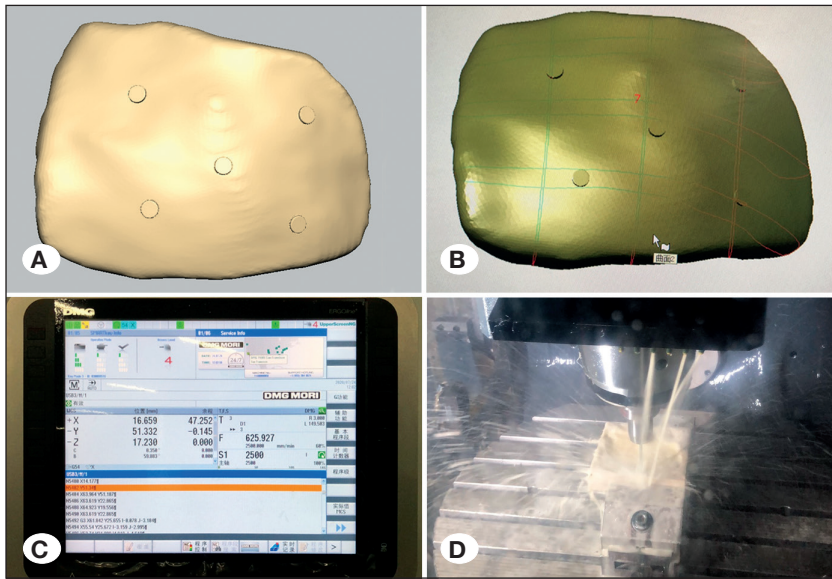
Figure 3: Manufacture process of the PEEK patch. **A)** 3D model data input to the design center for verification. **B)** 3D model data input to the control platform of the lathe. **C)** The processing parameters of patch molding were shown on the lathe. **D)** The manufacture process was performed in a closed space.
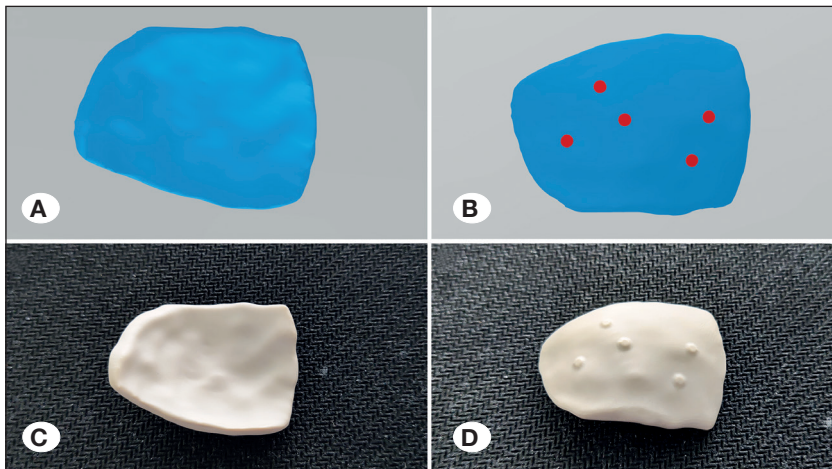

Figure 4: 3D-molded PEEK patch. **A, B)** 3D model of the extended patch. **C, D)** 3D-molded 1:1 PEEK patch.
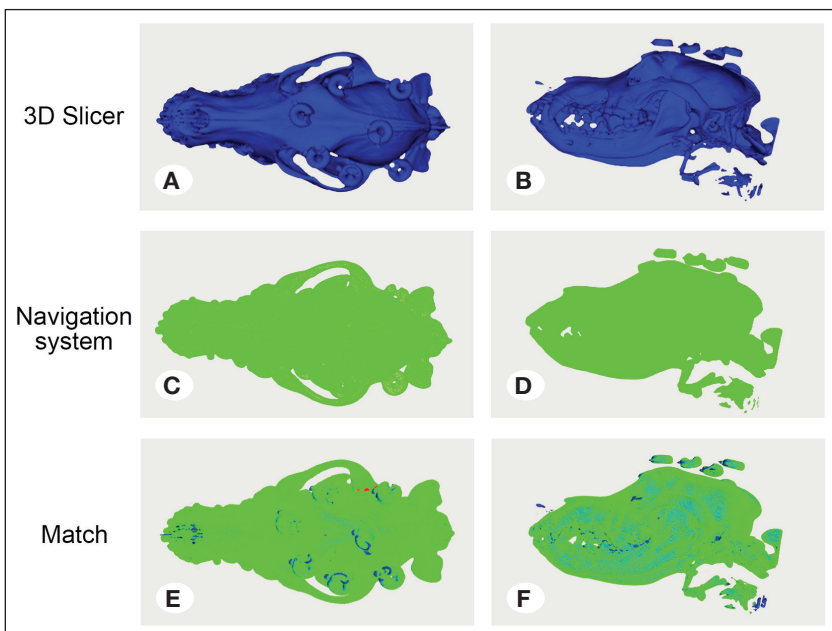

Figure 5: Coordinate transformation between 3D Slicer and the naviagtion system.
A, B) 3D reconstruction of dog skull in 3D Slicer.
C, D) Point cloud of dog skull in the navigation system. **E, F)** Overlap of the coordinates after transformation. **Left:** Superior aspect.
Right: Lateral aspect.

Using combined intraoperative navigation (Figure 6A, B) and real-time 3D reconstruction technology, we acquired the 3D skull defect model during the operation without an intraoperative CT scan (Figure 7A-F).

Through coordinate transformation and surface feature structure, the 3D-molded skull patch was registered precisely to the preoperative space image with navigation. Exact trimming could then be performed on the preformed extended patch after registration (Figure 8A-E).

Figure 6: Preoperative neuronavigation via surface markers on the dog. **A)** Navigation interface. **B)** Registration with surface markers on the skull.
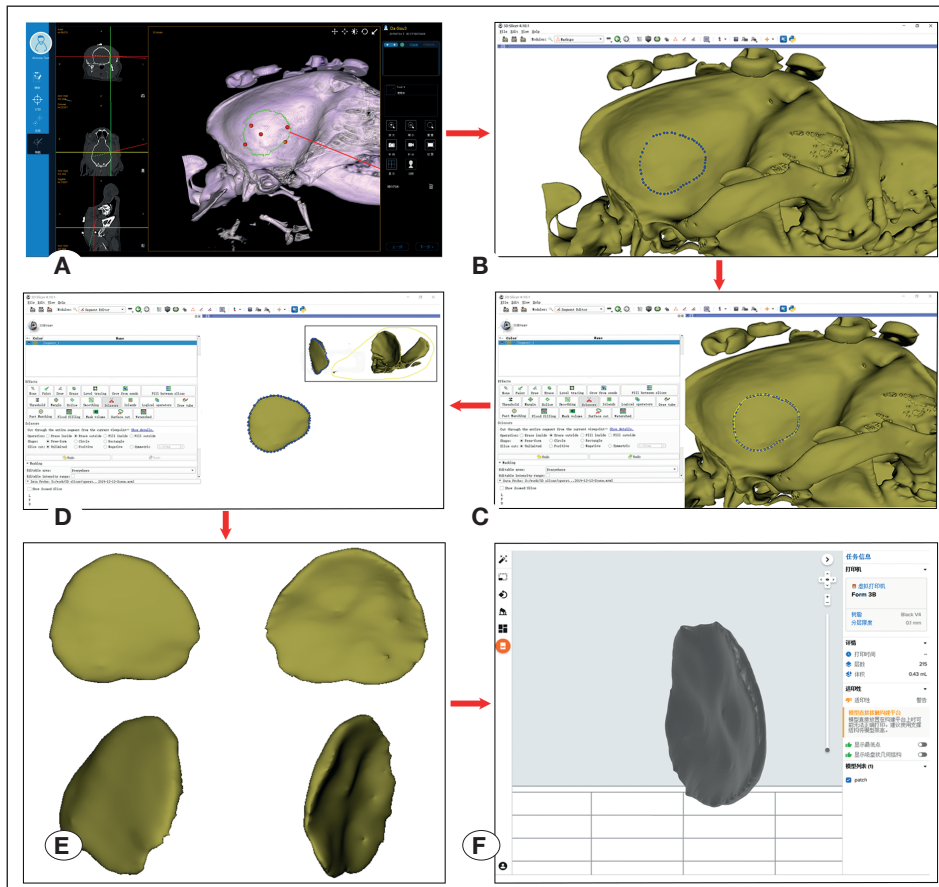

Figure 7: Intraoperative 3D modeling defect of the temporal bone. **A)** Actual temporal bone defect tracing. **B)** Coordinate transformation to the 3D Slicer. **C, D)** 3D model reconstruction of the actual temporal bone defect patch. **E, F)** 3D printing of the patch.

A postoperative blood test showed no evidence of infection. CT and MRI examination showed no displacement or absorption of the skull patch, no abnormal signal in the adjacent brain, and few epidural effusions (Figure 9 and 10A-F).

■ **DISCUSSION**

After decades of development, cranial vault remodeling is relatively mature. However, primary osseous repair of skull defects has caused problems for surgeons, especially when the defect is in the skull base or the area adjacent to it, such as the temporal bone. Ti mesh is a widely used material for repair, and most temporal bone defects can be successfully repaired with it.

With the progress of 3D molding technology, a perfectly matching patch can be prepared when the size of the defect is known preoperatively through a CT scan. 3D digital shaping Ti mesh prepared by lathe technology and injection molding with PMMA has been approved for clinical use (19). However, it is difficult to accurately estimate the resection range intraoperatively in primary repair when the lesion of the temporal bone is large and adjacent to the skull base. This often results in the need for secondary molding. Although a study has shown that the extended patient-specific 3D-molded Ti mesh can be intraoperatively trimmed and precisely fitted to restore normal contour (16), difficult tailoring and fixation near the skull base often leads to the upwarp of the material, unattractive appearance, and even Ti mesh exposure (12,22). Compared with autogenous bone, Ti mesh lacks sufficient rigidity and is susceptible to ambient temperature, which can create discomfort for the patient and cause artifacts in imaging examination (3).
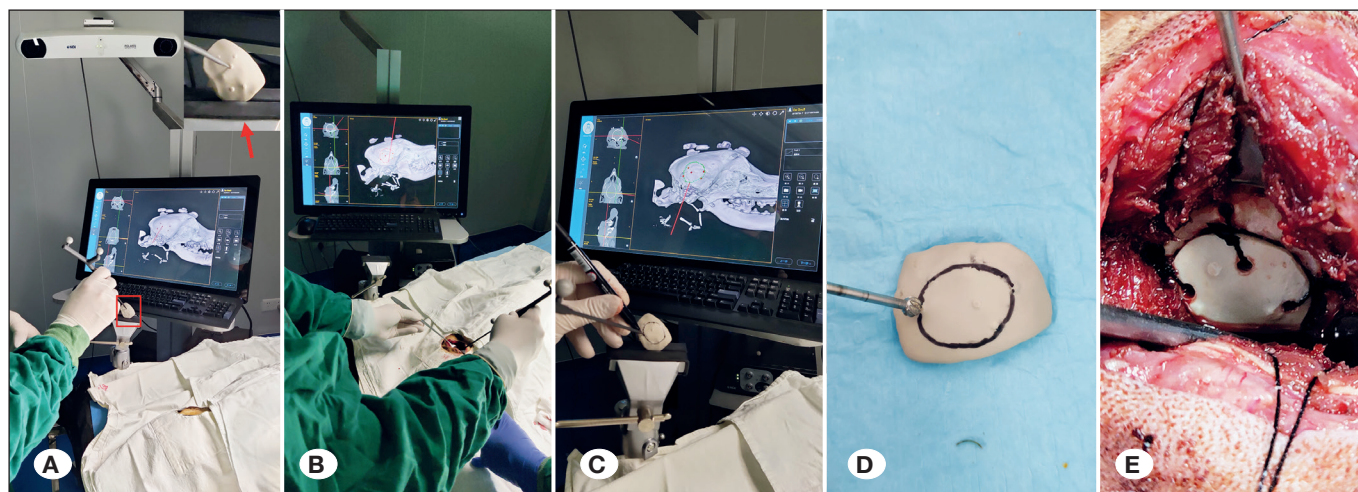

Figure 8: PEEK patch registration, trimming, and implantation. **A)** Patch (red arrow) registration. **B)** Actual profile of the skull base defect tracing. **C)** Duplication of the actual defect profile. **D)** Trimming the extended patch according to the path. **E)** Patch implantation and fixation.
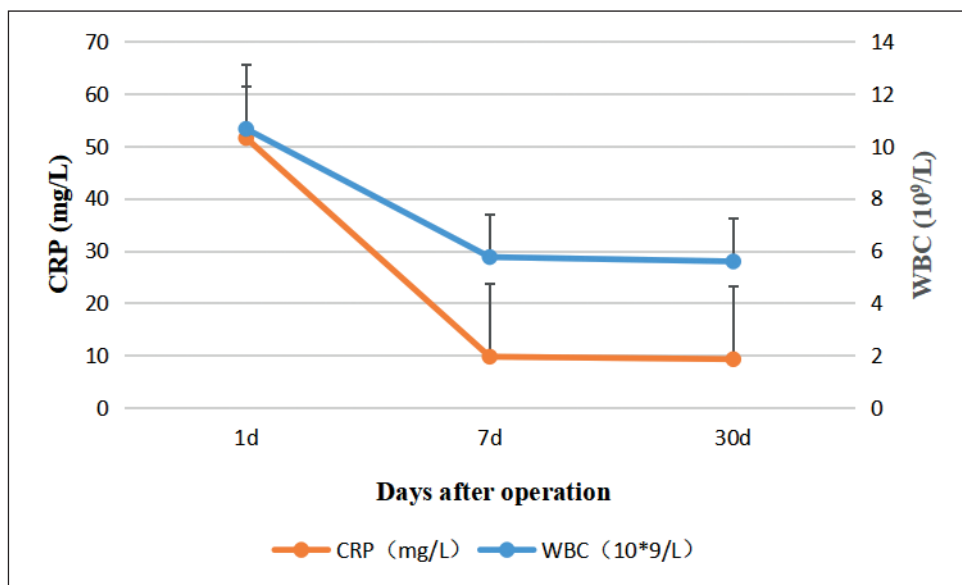

Figure 9: Postoperative blood test. White blood cells and C-reactive protein examination showed a mild inflammatory response at the early stage which returned to normal on day 7 and day 30.
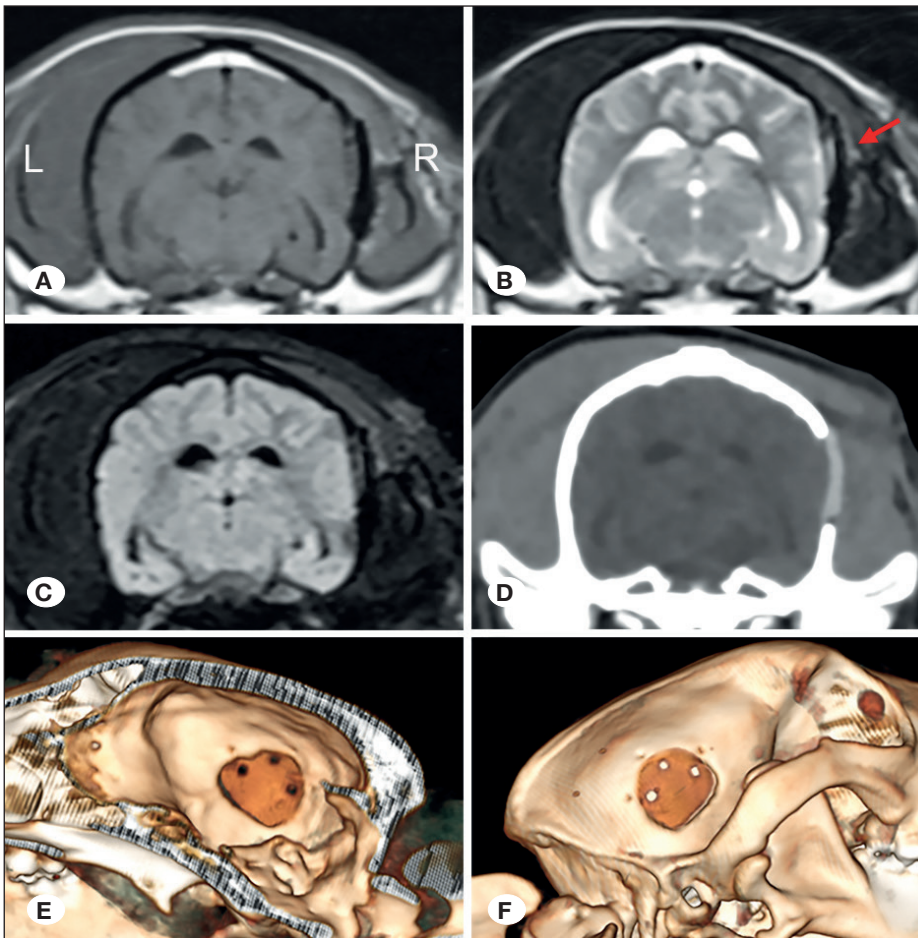
Figure 10: MRI and CT scans at 1 month postoperation**. A-C)** MRI showed no obvious secondary brain injury and few epidural effusions (red arrow). **D-F)** CT and 3D reconstruction showed no displacement or absorption of the skull patch. **CT:** computed tomography; **MRI:** magnetic resonance imaging.

PEEK is a popular synthetic thermoplastic polymer organic material with an elastic modulus more similar to that of bone than metals, with the added benefits of good biocompatibility, radiation resistance, stability, and no artifacts. In recent years, improvements in lathe technology have led to the development of a 1:1 individual skull patch, which has already been used in clinical cranioplasty (5,13). After simple training, it takes a technician less than 30 minutes to estimate the defect and design an extended patch model with feature markers. The average molding time for a 10 cm3 model processed with 0.01 mm precision is 45 minutes after the designed data are input into the automatic lathe workstation. The product is delivered in fewer than 3 days, including delivery time. The total time spent above will not delay the operation, as time can be saved in clinical use by completing a CT scan and a patch design before hospitalization. The high temperature sterilization resistance of PEEK is convenient for intraoperative use following a 15-minute autoclave sterilization. In addition, the preformed PEEK patch can be reprocessed intraoperatively by grinding, which creates an opportunity for remolding.

It is crucial to obtain the actual boundary of the defect for intraoperative patch reprocessing. However, skull base defect repair frequently involves irregular shapes and a narrow operating space, making precise tailoring difficult with only visual observation. Using coordinate transformation and intraoperative navigation, it is possible to accurately duplicate the boundary of the skull defect on the extended PEEK patch. Since the design of our extended patch model was performed using open-source 3D reconstruction software, it was necessary to finish the work of coordinates transformation between the 3D Slicer and the navigation system. ICP is a mature algorithm for coordinate transformation, and the result showed perfect matching via accurate calculation. With reference to a previous study, we built 5 identifiable characteristic landmarks to facilitate intraoperative patch registration (6). The registration could be finished without pointing to the subject's anatomy markers, as the coordinate information of the landmarks on the patch had been converted to the navigation system preoperatively. Scattered distribution of the landmarks can improve the accuracy and success rate of registration (8). After the registration of the PEEK patch, the coordinates of the dog, the navigation, and the patch were unified. Real-time tracing and display of the skull defect boundary and trimming of the PEEK patch then proceeded successfully. A perfectly matched patch prepared by the described method enabled us to perform an anatomical repair.

In recent years, 3D printing has been used to prepare 3D skull prostheses (2,15). Although no approved 3D-printed material

for skull repair yet exists, this will be a potential development direction for primary skull defect repair as printing technology and materials improve. In another experiment, perfect repair of a cadaver skull was achieved through the combination of a preoperative individualized 3D-printed mold and injection of water-soluble PMMA (7). However, that process was completed after the skull defect range had been determined. Obtaining an actual model of the defect is critical for intraoperative 3D printing when faced with an unpredictable defect. Although a mobile CT scan is very useful for obtaining the exact profile of the actual defect intraoperatively, these systems are expensive, radioactive, and may not be available in many hospitals (4). By means of navigation and coordinate system transformation, it is possible to obtain a 3D model of the actual defect using 3D Slicer for 3D printing without the intraoperative CT. This method is safe, convenient, and time-saving.

Our in vivo study verified the validity of a primary repair of temporal bone defects in dogs, solved the problem of implant materials, and precisely mapped a defect model for reconstruction. Postoperative examinations showed no rejection or inflammatory reaction to the patch, which was perfectly matched to the shape of the defect. Due to its high hydrophobicity and smooth surface, PEEK has poor adhesion strength with soft tissue and the capacity to osseointegrate, which can lead to the epidural effusion seen with other polymer materials (9). As to be expected, we found slight epidural effusions in our study. Porous structures and the hydrophobic coating of the PEEK patch were designed to reduce the occurrence of effusion and increase the adherence to the adjacent tissue (1,18,23). The overall costs of this skull reconstruction system mainly related to navigation, 3D reconstruction, and the use of PEEK. Although neuronavigation is still relatively expensive, it is worth using due to improvements in the efficacy of surgery and reduced complications. In our department, the 3D reconstruction process is currently based on an open-source system. We intend to integrate the process into our home navigation planning system, which will eliminate coordinate conversion steps and reduce costs. Due to waste during processing and the shortage of raw materials, the current price of PEEK patches is high and constitutes the greatest burden on patients. To address this, we are developing PEEK 3D printing and increasing our supply to reduce the cost of implantation.

The present study has some limitations. First, this model cannot reflect the complexity of all temporal bone defects, such as those of the lateral skull base. Second, we traced out the route on the patch using manual control, which may reduce the precision of trimming. Mechanical linkage and remote-controlled devices would solve this problem. We were able to acquire the actual profile once the defect was identified prior to lesion resection, dural closing, and trimming of the patch in a separate place. Finally, the research period was not sufficiently long to determine the distant rejection of the implant by the host. We expect to investigate the effects of its clinical application further.

■ CONCLUSION

The combination of neuronavigation, 3D reconstruction technology and customized individual PEEK patches can assist surgeons in performing accurate primary repair of bone defects of the skull and help accelerate patient recovery after surgery.

■ ACKNOWLEDGEMENTS

AUTHORSHIP CONTRIBUTION

Study conception and design: JG, YG
Data collection: YJX, HYH, BYZ, TCH
Analysis and interpretation of results: YJX, LL
Draft manuscript preparation: JG, MTL
Critical revision of the article: JG, YG
Other (study supervision, fundings, materials, etc...): RQY
All authors (YG, YJX, HYH, MTL, LL, BYZ, TCH, RQY, YG) reviewed the results and approved the final version of the manuscript.

■ REFERENCES

1. Carpenter RD, Klosterhoff BS, Torstrick FB, Foley KT, Burkus JK, Lee CSD, Gall K, Guldberg RE, Safranski DL: Effect of porous orthopaedic implant material and structure on load sharing with simulated bone ingrowth: A finite element analysis comparing titanium and PEEK. J Mech Behav Biomed Mater 80:68-76, 2018

2. Chamo D, Msallem B, Sharma N, Aghlmandi S, Kunz C, Thieringer FM: Accuracy assessment of molded, patient-specific polymethylmethacrylate craniofacial implants compared to their 3D printed originals. J Clin Med 9(3):832, 2020

3. Chaskis E, Sadeghi N, De Witte O, Lefranc F: Neurosurgical device implantation for neuro-oncological patients: What to avoid? Technical note. World Neurosurg 124:298-303, 2019

4. Conley DB, Tan B, Bendok BR, Batjer HH, Chandra R, Sidle D, Rahme RJ, Adel JG, Fishman AJ: Comparison of intraoperative portable ct scanners in skull base and endoscopic sinus surgery: Single center case series. Skull Base 21(4):261-270, 2011

5. Eolchiyan SA: Complex skull defects reconstruction with titanium and polyetheretherketone (PEEK) implants. Zh Vopr Neirokhir Im N N Burdenko 78(4):3-13, 2014

6. Essayed WI, Unadkat P, Hosny A, Frisken S, Rassi MS, Mukundan S, Weaver JC, Al-Mefty O, Golby AJ, Dunn IF: 3D printing and intraoperative neuronavigation tailoring for skull base reconstruction after extended endoscopic endonasal surgery: Proof of concept. J Neurosurg 130(1):248-255, 2018

7. Evins AI, Dutton J, Imam SS, Dadi AO, Xu T, Cheng D, Stieg PE, BernardoA: On-demand intraoperative 3-dimensional printing of custom cranioplastic prostheses. Oper Neurosurg (Hagerstown) 15(3):341-349, 2018

8. Fitzpatrick JM, West JB, Maurer CR Jr: Predicting error in rigid-body point-based registration. IEEE Trans Med Imaging 17:694-702, 1998

9. Kerr RG, Hearst MJ, Samy RN, van Loveren HR, Tew Jr JM, Pensak ML, Theodosopoulos PV: Delayed extrusion of hydroxyapatite cement after transpetrosal reconstruction. Neurosurgery 64(3):527-531; discussion 531-532, 2009

10. Kwiecien GJ, Sinclair N, Coombs DM, Djohan RS, Mihal D, Zins JE: Long-term effect of cranioplasty on overlying scalp atrophy. Plast Reconstr Surg Glob Open 8(8):e3031, 2020

11. Malivuković A, Novaković N, Lepić M, Minić L, Stepić N, Đorđević B, Rasulić L: Cranial reconstruction with prefabricated 3D implant after a gunshot injury: A case report. Vojnosanit Pregl 73(8):783-787, 2016

12. Mikami T, Miyata K, Komatsu K, Yamashita K, Wanibuchi M, Mikuni N: Exposure of titanium implants after cranioplasty: A matter of long-term consequences. Interdisciplinary Neurosurgery 8:64-67, 2017

13. Nguyen PD, Khechoyan DY, Phillips JH, Forrest CR: Custom CAD/CAM implants for complex craniofacial reconstruction in children: Our experience based on 136 cases. J Plast Reconstr Aesthet Surg 71(11):1609-1617, 2018

14. Oliver JD, Banuelos J, Abu-Ghname A, Vyas KS, Sharaf B: Alloplastic cranioplasty reconstruction: A systematic review comparing outcomes with titanium mesh, polymethyl methacrylate, polyether ether ketone, and norian implants in 3591 adult patients. Ann Plast Surg 82(5S Suppl 4): S289-S294, 2019

15. Pijpker PAJ, Wagemakers M, Kraeima J, Vergeer RA, Kuijlen JMA, Groen RJM: Three-dimensional printed polymethylmethacrylate casting molds for posterior fossa reconstruction in the surgical treatment of chiari i malformation: Technical note and illustrative cases. World Neurosurg 129: 148-156, 2019

16. Sunderland IR, Edwards G, Mainprize J, Antonyshyn O: A technique for intraoperative creation of patient-specific titanium mesh implants. Plast Surg (Oakv) 23(2):95-99, 2015

17. Thien A, King NKK, Ang BT, Ernest Wang E, Ng I: Comparison of polyetheretherketone and titanium cranioplasty after decompressive craniectomy. World Neurosurg 83(2):176-180, 2015

18. Torstrick FB, Safranski DL, Burkus JK, Chappuis JL, Lee CSD, Guldberg RE, Gall K, Smith KE: Getting PEEK to stick to bone: The development of porous PEEK for interbody fusion devices. Tech Orthop 32(3):158-166, 2017

19. Wu CT, Lee ST, Chen JF, Lin KL, Yen SH: Computer-aided design for three-dimensional titanium mesh used for repairing skull base bone defect in pediatric neurofibromatosis type 1. A novel approach combining biomodeling and neuronavigation. Pediatr Neurosurg 44(2): 133-139, 2008

20. Yoshioka N, Tominaga S: Titanium mesh implant exposure due to pressure gradient fluctuation. World Neurosurg 119: e734-e739, 2018

21. Zanetti D, Nassif N: Transmastoid repair of minor skull base defects with flexible hydroxyapatite sheets. Skull Base 13(1):1-11, 2003

22. Zhang Q, Yuan Y, Li X, Tong Sun T, Zhou Y, Yu H, Guan J: A large multicenter retrospective research on embedded cranioplasty and covered cranioplasty. World Neurosurg 112: e645-e651, 2018

23. Zhao X, Xiong D, Liu Y: Improving surface wettability and lubrication of polyetheretherketone (PEEK) by combining with polyvinyl alcohol (PVA) hydrogel. J Mech Behav Biomed Mater 82:27-34, 2018